Japan-Canada Joint Seminar on Advanced Electron Microscopy and its Application

『日本-カナダ先端分析顕微鏡合同セミナー』

Third Japan-Canada

Microscopy Societies Joint Symposium 2022

第3回　日本-カナダ

顕微鏡学会交流シンポジウム　2022

November 4 - 5, 2022

at

Kawasaki Sukenobu Memorial Lecture Hall
Kawasaki University of Medical Welfare, Kurashiki, Okayama, Japan

Japanese Society of Microscopy (JSM)

Microscopy Society of Canada (MSC)

Third Japan-Canada Microscopy Societies Joint Symposium 2022

Time (Tokyo)	Friday, November 4	Saturday, November 5	Sun. Nov. 6	Time (Toronto)	Time (Edmonton)
7:50 ~ 8:00	Connecting / 7:55 ~ Opening	Connecting		18:50 ~ 19:00	16:50 ~ 17:00
8:00 ~ 8:20	Bio-01 Canada, (Keynote) M. Hendzel	Mate-07 Canada, (Keynote) A. M. Blackburn		19:00 ~ 19:20	17:00 ~ 17:20
8:20 ~ 8:40				19:20 ~ 19:40	17:20 ~ 17:40
8:40 ~ 9:00	Bio-02 Japan, H. Hioki	Mate-08 Canada, J. Howe		19:40 ~ 20:00	17:40 ~ 18:00
9:00 ~ 9:20	Bio-06 Japan, H. Yamanishi	Mate-09 Japan, D. Morikawa		20:00 ~ 20:20	18:00 ~ 18:20
9:20 ~ 9:40	Bio-04 Japan, (Keynote) K. Toida	Mate-10 Canada, N. Braidy		20:20 ~ 20:40	18:20 ~ 18:40
9:40 ~ 10:00		Mate-11 Japan, N. Shibata		20:40 ~ 21:00	18:40 ~ 19:00
10:00 ~ 10:10	Short Break	Closing ~ 10:05		21:00 ~ 21:10	19:00 ~ 19:10
10:10 ~ 10:30	Bio-05 Japan, S. Hayashi		The 65th JSM Symposium	21:10 ~ 21:30	19:10 ~ 19:30
10:30 ~ 10:50	Bio-03 Canada, J. Ortega	The 65th JSM Symposium		21:30 ~ 21:50	19:30 ~ 19:50
10:50 ~ 11:20	BINA-01 Canada, C. M. Brown			21:50 ~ 22:20	19:50 ~ 20:20
11:20 ~ 11:40	Mate-01 Canada, R. F. Egerton			22:20 ~ 22:40	20:20 ~ 20:40
11:40 ~ 12:00	Mate-02 Japan, T. Ishii			22:40 ~ 23:00	20:40 ~ 21:00
12:00 ~ 13:00	Lunch			23:00 ~ 24:00	21:00 ~ 22:00
13:00 ~ 13:20	Mate-03 Japan, T. Shimojima			24:00 ~ 24:20	22:00 ~ 22:20
13:20 ~ 13:40	Mate-04 Japan, H. Nakajima			24:20 ~ 24:40	22:20 ~ 22:40
13:40 ~ 14:00	Mate-05 Japan, L. Peng			24:40 ~ 25:00	22:40 ~ 23:00
14:00 ~ 14:20	Mate-06 Japan, (Keynote) H. Kurata			25:00 ~ 25:20	23:00 ~ 23:20
14:20 ~ 14:40				25:20 ~ 25:40	23:20 ~ 23:40
14:40 ~ 15:00				25:40 ~ 26:00	23:40 ~ 24:00
15:00 ~ 16:00	Move to the reception venue, "Ohara Museum of Art"			26:00 ~ 27:00	24:00 ~ 25:00
16:00 ~				27:00 ~	25:00 ~

【Preface】

Dear Participants,

On behalf of the Organization Committee, we warmly welcome you to attend the third Japan-Canada Microscopy Societies Joint Symposium 2022, supported financially by the Japan Society for the Promotion of Science (JSPS). Since 2020, the joint symposiums have been held with the aim of deepening mutual exchanges between the Japanese Society of Microscopy (JSM) and the Microscopy Society of Canada (MSC). The 1st (held in Osaka in May 2020) and the 2nd (held in November 2021 at the University of Alberta) was held on-paper and on-line due to the COVID-19 pandemic. The 3rd Japan-Canada Joint Symposium on Advanced Analytical Microscopy will be held in Kurashiki, Okayama in November 2022. The general purpose of this symposium is to provide a great opportunity for researchers, especially young researchers, of JSM and MSC to communicate with world-leading experts and discuss the next generation of microscopy.

In this symposium we will invite participants on a wide range of topics, including not only electron microscopes but also ion microscopes, new equipment and technologies, and data processing methods and their applications that have made rapid progress in recent years. It also aims to advance microscopy and further development of microscope technology through direct exchanges between Japanese and Canadian researchers and the two societies. Furthermore, in terms of mutual exchanges at the academic society level, we will take advantage of the characteristics of both societies to conduct exchanges not only in the fields of metals and semiconductors, but also in the fields of medicine and biology.

Unfortunately, due to the travel limitation imposed by the COVID-19 pandemic, it is a pity that this year all the sessions in Canadian side will be held in the online mode, although the committee did try our best for organizing an on-site conference. We sincerely wish this symposium will be held in-person next year!

Finally, we would like to thank all the researchers who participated

in this symposium, Dr. Kazunori Toida, chairman of the 65th symposium of JSM, and the members of the organizing committee of the 65th symposium for their support in planning this symposium, and for their cooperation in this project. Also, we would like to thank all of you who attended in this symposium. We hope that mutual exchanges between the Japanese and Canadian microscopy societies will continue in the future.

On behalf of all the organizers
Shigeo Mori (Osaka Metropolitan University)

【Greetings】

Yuichi Ikuhara, (University of Tokyo)
President of The Japanese Society of Microscopy

This is the third symposium for bilateral exchange between the Japanese Society of Microscopy (JSM) and the Microscopy Society of Canada (MSC). This time, we planned to hold this symposium in conjunction with the 65th symposium of the JSM, which will be held at Kawasaki University of Medical Welfare, Kurashiki city in Japan. This symposium is also in line with the "Initiative toward Internationalization" that JSM is currently actively promoting. In addition, the theme of the symposium "Microscopy which is contributed to the state-of-the-art science" is very timely and useful for our field. When the first symposium was planned three years ago, with the support of the Japan Society for the Promotion of Science (JSPS), it was hoped that it would promote close exchanges and joint research between microscopy societies between Japan and Canada. However, due to the spread of the new coronavirus infection at the beginning, the first symposium was held on paper. On the other hand, since there was a strong request from the parties concerned to keep the project of this important symposium, the 2nd symposium was successfully held virtually. This is the 3rd time, following on from that, and the organizers have set up lectures on cutting-edge science in the Biological Science Session and the Materials Science Session in a well-balanced manner. It will be held in a hybrid system from Kawasaki University of Medical Welfare. I would like to thank Prof. Shigeo Mori chairman of the third Japan-Canada Microscopy Societies Symposium, all members of the organizing committee, Prof. Kazunori Toida, and Dr. Ken Harada for their big effort and supporting this symposium. I also would like to express my heartfelt gratitude to Prof. Kathryn Grandfield, President of Microscopy Society of Canada, and to the members of the organizing committee, Prof. Marek Malac and Dr. Misa Hayashida, on the Canadian side. I really hope that the continuation of this symposium will further develop exchanges between microscopy societies in two countries. I also hope that the next symposium will be held face-to-face in Canada or Japan.

【Greetings】

Kathryn Grandfield, (McMaster University)
President of Microscopy Society Canada

On behalf of the Microscopy Society of Canada- Société du Microscopie du Canada (MSC-SMC), I am honoured to welcome you to the Third Japan-Canada Microscopy Societies Joint Symposium held at the Kawasaki University of Medical Welfare in Kurashiki, Okayama, Japan. Together, our two societies have been pushing the frontiers of electron microscopy with this exciting conference, now in its third year.

This year's meeting focused on, "Advanced Electron Microscopy and its Application" will bring together the latest developments and eminent speakers from across Japan and Canada presenting ground-breaking research spanning techniques, such as correlative electron microscopy, electron diffraction, analytical techniques, in situ electron microscopy, ultrafast microscopy and electron tomography for broad applications spanning both the Materials and Biological Sciences.

This annual meeting has proven to be a fruitful opportunity for scientific collaboration and exchange between our two societies, and its continued success is evidence of the advancements in microscopy our societies are making together.

I extend my deepest thanks to the sponsoring organizations and volunteer organizers in Canada and Japan who have worked so tirelessly to bring you this exciting meeting. Thank you to my fellow society, the JSM, for extending the generous invitation to join you again in our third year.

We look forward to welcoming you to Canada next year for the 50th Anniversary of the MSC-SMC and another stimulating Japan-Canada meeting. I give my warmest welcome to all attendees, in-person or virtually, and wish you a good scientific meeting.

【Scientific Program】

Day 1　(Tokyo time: Friday, November 4, 2022)

Opening　07:55 – 08:00

Biological Science Session

Bio-01　08:00 – 08:40

Michael J.Hendzel (University of Alberta)

The development of 3-channel imaging methods to discriminate biomolecules in interphase nuclei

Bio-02　08:40 – 09:00

Hiroyuki Hioki, (Juntendo University)

A multiscale imaging from macroscopic to nanoscopic levels with a tissue clearing method, Sca*l*eSF

Bio-06　09:00 – 09:20

Haruyo Yamanishi (Shiseido Co., Ltd.)

Morphological changes of intracellular organelles during terminal differentiation of the epidermis

Bio-04　09:20 – 10:00

Kazunori Toida (Kawasaki Medical School)

Multimodal regulation of olfactory neural circuit, as revealed by correlated laser and volume electron microscopy, ultra-high voltage electron microscopy, and electron tomography

Short Break　10:00 – 10:10

Bio-05　10:10 – 10:30

Shuichi Hayashi (Kawasaki Medical School)

Developmental analysis of complex synaptic connections by correlative light and electron microscopy

Bio-03　10:30 – 10:50

Joaquin Ortega (McGill University)

Getting ahead of the next pandemic: When antibiotics stop working

10:50 – 11:20

Claire M. Brown (McGill University)

National and international bioimaging networks

Materials Science Session

Mate-01　11:20 – 11:40

Ray F. Egerton (University of Alberta)

TEM of thick polymer or biological specimens

Mate-02　11:40 – 12:00

Tomohito Ishii (Osaka University)

Improving spatial resolution in rapid electron tomography for hundreds-nm-sized 3D materials

Lunch　12:00 – 13:00

Mate-03　13:00 – 13:20

Takahiro Shimojima (RIKEN)

Magnetic dynamics probed by ultrafast transmission electron microscopy

Mate-04　13:20 – 13:40

Hiroshi Nakajima (Osaka Metropolitan University)

Ferroelectric nanostructures observed by transmission electron microscopy

Mate-05　13:40 – 14:00

Licong Peng (RIKEN)

In-situ L-TEM observations of magnetic skyrmion and antiskyrmion dynamics

Mate-06　14:00 – 14:40

Hiroki Kurata (Kyoto University)

Electronic state analysis using monochromated STEM-EELS

Day 2   (Tokyo time: Saturday, November 5, 2022)

Materials Science Session

Mate-07   08:00 – 08:40

Arthur M. Blackburn (University of Victoria)

Accessing sub-Ångström ptychographic information in a scanning electron microscope below 30 kV

Mate-08   08:40 – 09:00

Jane Howe (University of Toront)

Automatic quantification of microplastic fibres in scanning electron micrographs

Mate-09   09:00 – 09:20

Daisuke Morikawa (Tohoku University)

Local structure analysis of interface and polar nano domains using convergent-beam electron diffraction

Mate-10   09:20 – 09:40

Nadi Braidy (University of Sherbrooke)

Interpretation of 3D EDX maps: multivariate analysis and deep learning hybrid approach

Mate-11   09:40 – 10:00

Naoya Shibata (University of Tokyo)

Atomic resolution magnetic field imaging by scanning transmission electron microscopy

Closing   10:00 – 10:05

Continue to the 65th JSM Symposium

https://conference.wdc-jp-com/microscopy/sympo/65th/

【Abstracts】

Day 1   **(Tokyo time: Friday, November 4, 2022)**

Biological Science Session

The development of 3-channel imaging methods to discriminate biomolecules in interphase nuclei

Hilmar Strickfaden, Natnael Abate, and Michael J. Hendzel

[1] Departments of Cell Biology and Oncology

[2] Faculty of Medicine and Dentist

[3] University of Alberta, Edmonton, Canada T6G 1Z2

[*] mhendzel@ualberta.ca

The ability to image cell structures at molecular resolution makes transmission electron microscopy the technique best-suited to study the molecular organization of cells. Much of what we know about the organization of the cytoplasm is derived from transmission electron microscopy studies. Although fluorescence microscopy progresses increasingly closer to transmission electron microscopy resolution, the technique is limited by the intrinsic inability to identify molecules without the use of exogenous fluorescent labels. Thus, molecules and structures that are not labelled cannot be distinguished from a complete absence of molecules/structures in that space. Transmission electron microscopy is mass sensitive and can contrast all biological structure. However, the absence of colour has made it very difficult to compare distributions and relationships of two or more types of biomolecules, at the same time thus limiting functional analysis. Discrimination of structures relies upon morphological differences rather than on contrast. This becomes problematic in the nucleoplasm where fibrillar material could be chromatin, RNA, or protein. While specific stains exist to discriminate amongst these molecules, they cannot be used in combination because conventional transmission electron microscopy is a single-channel technology. A potential path around this barrier is presented by electron spectroscopic imaging (ESI). ESI can map distributions of chemical elements within an ultra-thin section. We have previously shown that the combination of nitrogen and phosphorus maps can be highly informative on the interpretation of nuclear structures. A disadvantage of this approach was that osmium tetroxide staining significantly impaired the acquisition of the phosphorus maps. Consequently, we were unable to preserve biological membranes. In this study, we made preserved membranes with potassium permanganate and imaged them with manganese, resulting in 3-color images. In separate 3-color experiments, we used potassium permanganate to contrast diaminobenzidine polymerized by

photooxidation or using a singlet-oxygen generating enzyme to identify specific molecules that we have incorporated enzymatic tags (APEX2) or fluorescently labelled molecules to polymerize DAB at the location of the molecule of interest. Finally, we have used RNA-specific staining to generate 3 color maps where RNA can be distinguished from DNA. This enables the localization of RNA relative to the underlying chromatin and will significantly advance our understanding of the organization of RNA within the interphase nucleus.

A Multiscale imaging from macroscopic to nanoscopic levels with a tissue clearing method, Sca*l*eSF.

Hiroyuki Hioki[1,2,3,*], Kenta Yamauchi[1,2], Takahiro Furuta[4]

[1]Department of Neuroanatomy, Juntendo University Graduate School of Medicine
[2]Department of Cell Biology and Neuroscience, Juntendo University Graduate School of Medicine
[3]Department of Multi-Scale Brain Structure Imaging, Juntendo University Graduate School of Medicine
[4]Department of Oral Anatomy and Neurobiology, Graduate School of Dentistry, Osaka University

[*]h-hioki@juntendo.ac.jp

The mammalian brain contains a heterogeneous mixture of billions of neurons with trillions of synapses. Connectomics, a description of wiring diagram of the nervous system, is fundamental for understanding how a neural circuit processes information and generates behavior (Lichtman and Sanes, Curr Opin Neurobiol, 2008). While neurons elaborate highly specialized processes that can span over a meter in length, synapses that connect neurons are several hundred nanometers in size. Thus, the imaging scale required for deciphering brain-wide connectivity exceeds several orders of magnitude.

Our study overcomes the technical requirements required for whole-brain and nanoscale imaging by coupling a tissue clearing method with successive LM/EM imaging (multi-scale LM/EM neuronal imaging). We have established an imaging pipeline that enables correlative light and electron microscopy (CLEM) in optically cleared tissues in this study (**Fig**). Our multi-scale neuronal imaging makes it possible to describe synaptic connectivity of brain-wide circuits by simultaneous interrogation of the neural circuit structure mapped in optically cleared brain tissues, and synaptic connectivity imaged with EM in a reasonable amount of time, without the need for specialized equipment. Our study has expanded the applicability of tissue clearing techniques from LM to EM by developing an ultrastructurally-preserved tissue clearing method, Sca*l*eSF, and implementing LM/EM dual labeling that remained stable in the clearing protocol. We believe that our technique will contribute to our understanding of brain-wide connectivity beyond the reach of current connectomic analyses with a single imaging modality.

References:

[1] Furuta T, Yamauchi K, Okamoto S, Takahashi M, Kakuta S, Ishida Y, Takenaka A, Yoshida A, Uchiyama Y, Koike M, Isa K, Isa T, *Hioki H. (2022) Multi-scale light microscopy/electron microscopy neuronal imaging from brain to synapse with a tissue clearing method, Sca*l*eSF. *iScience*. **25**:103601.

[2] Yamauchi K, Furuta T, Okamoto S, Takahashi M, Koike M, *Hioki H. (2022) Protocol for multi-scale light microscopy/electron microscopy neuronal imaging in mouse brain tissue. *STAR Protocols*. **3**:101508.

[3] Yamauchi K, Okamoto S, Takahashi M, Koike M, Furuta T, *Hioki H. (2022) A Tissue Clearing Method for Neuronal Imaging from Mesoscopic to Microscopic Scales. *J Vis Exp*. 183:e63941.
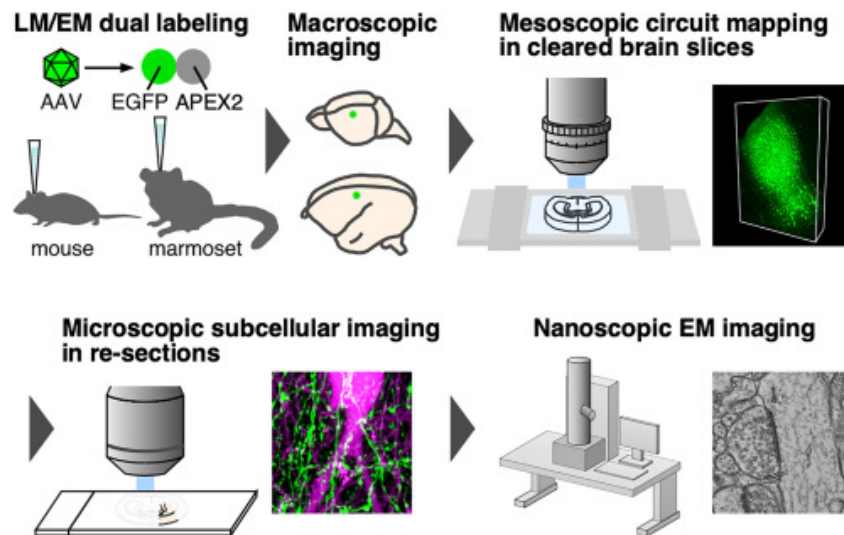
Fig. Multi-scale LM/EM neuronal imaging pipeline. Multi-scale neuronal imaging incorporates (1) macroscopic observation, (2) mesoscopic circuit mapping in cleared brain slices, (3) microscopic subcellular imaging in re-sections, and (4) nanoscopic EM imaging. Mouse and marmoset neurons are labeled with an AAV vector carrying a fluorescent and electron-dense genetically encoded CLEM probe, EGFP-APEX2.

Morphological Changes of Intracellular Organelles during Terminal Differentiation of the Epidermis

Haruyo Yamanishi（山西治代）[1*], Akemi Ishida-Yamamoto (山本明美) [2]

[1] Shiseido Co., Ltd. MIRAI Technology Institute, 1-2-11, Takashima, Nishi-ku, Yokohama, Kanagawa, 220-0011, Japan.

[2] Department of Dermatology, Asahikawa Medical University, 1-1-1. Higashi-Ni-Jyo, Midorigaoka, Asahikawa, Hokkaido,078-8510, Japan

*haruyo.yamanishi@shiseido.com

Skin is the largest tissue in our body and plays an important role in barrier functions through the differentiation of keratinocytes. Intercellular lipids are released from lamellar granules (LGs) and prevent water loss. LGs are small organelles found in the cytoplasm of stratum granulosum (SG). LGs have been observed as oval-shaped vesicles or vesicular tubular structures on electron micrograph, but the three-dimensional (3D) structure of LG of the epidermis is unclear due to the technical limitations of the previously applied microscopy techniques.

Recently, many 3D ultrastructural analyses by scanning electron microscopy (SEM), which generates high resolution and back scattered images resembling transmission electron micrographs, have been reported. This technology, called block face imaging, is applied in several tissues including brain, kidney and testis, and expected to be evolved rapidly.

In this study, we aimed to elucidate the 3D structures and spatial distributions of LGs in normal human skin by focused ion beam-SEM (FIB-SEM) technique (Fig. 1). The FIB-SEM images indicated that LGs fused the cellular membrane in the most superficial layer of the SG. LGs in the second granular (SG2) layer was not only localized in the cytoplasm but also secreted into the intercellular space [1]. In contrast, LGs was maintained in the cytoplasm of the third granular layer. Trans-Golgi network (TGN) was visualized spreading into the cytoplasm with branched structures and connected to the vesicles of LGs in the SG2 layer [2]. These results suggest that LGs mature along with keratinocyte differentiation, and that the changes in LGs morphology associated with the SG2 layer represent an important step preceding LGs fusion with the cell membrane. We consider that further research for the 3D structure of LGs and TGN could elucidate pathological mechanisms of skin diseases which are associated with LGs.

References:

[1] Yamanishi H., Soma T., Ishida-Yamamoto A*., Kenbikyo,* (2019) Vol. 54, p.39-43

[2] Yamanishi H., Soma T., Kishimoto J., Hibino T., Ishida-Yamamoto A., *J Invest Dermatol.* (2019) Vol. 139 (2) p.352-359.
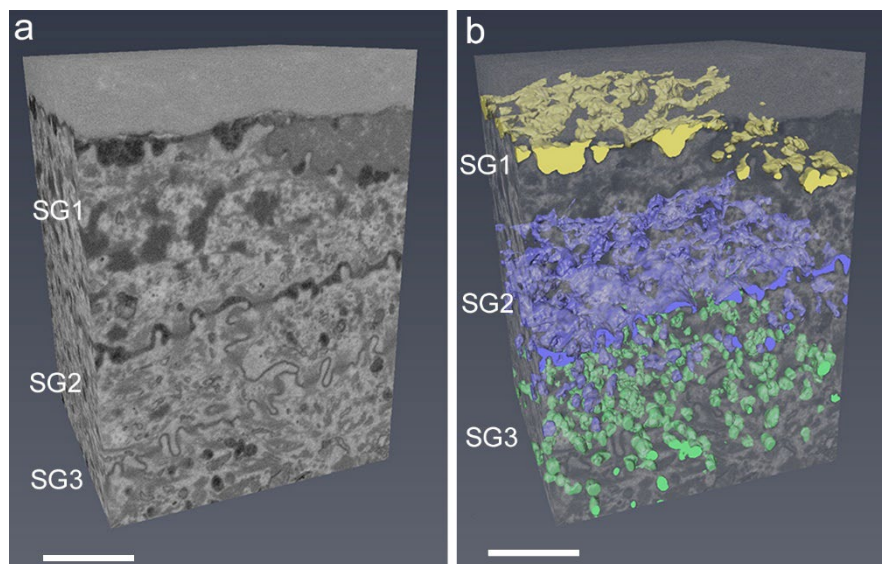
Fig.1　The distribution of lamellar granules in human epidermis. Adapted and translated from "Three-dimensional ultrastructural analysis of lamellar granules and trans-Golgi network in stratum granulosum by focused ion beam scanning electron microscopy," by Yamanishi H., et al., 2019, Kenbikyo, 54, p.39-43.

Multimodal regulation of olfactory neural circuit, as revealed by correlated laser and volume electron microscopy, ultra-high voltage electron microscopy, and electron tomography

Kazunori Toida[1,2,3*],

Sawa Horie[1], Keita Satoh[1], Nobuaki Matsuda[3,4], Yukari Minami[1,5], Satoshi Ichikawa[2], Shuichi Hayashi[1], Emi Kiyokage[4]

[1]Department of Anatomy, Kawasaki Medical School

[2]Research Center for Ultra-high Voltage Electron Microscopy, Osaka University

[3]Bio-imaging Unit, Central Research Institute, Kawasaki Medical School

[4]Department of Medical Technology, Kawasaki University for Medical Welfare

[5]Department of Neurosurgery, Kawasaki Medical School

[*]toida@med.kawasaki-m.ac.jp

We have been examining the olfactory bulb (OB), the primary center of the olfactory system, as an attractive model for analyzing basic structure of the neural circuit in the brain. The OB is organized by laminar structure containing neuronal organization with rich in chemical substances. These characteristic features are observed beyond animal species and thus further enable us to do variable microscopic experiments (Ref.1). At the outset, I would like to introduce just briefly the background of our research (Ref.1), followed by integrative morphological research so far analyzed by correlative laser and volume electron microscopy (serial-sectioning/reconstruction) for synaptic organization of the OB (Ref.2-4). Urgent questions raised in these series of our studies are how the OB is regulated by variable factors (Fig.1), and we need to establish anatomical basis for multimodal regulation of the neural circuit of the OB. To address, we have succeeded to label the OB neurons selectively by transgenic and/or genetic induction to apply for microscopic analyses we have been consistently performing (Ref.5-8, Fig.2).

Here, I would like to show our findings and let us consider all together developing progress and possibility in recently advanced microscopy, such as quantitative analyses by ultra-high voltage electron microcopy, electron tomography (Fig.3-5) and network tele-microscopy, to well understand the structure and function of the brain.

References:

[1] Toida K   *Anat Sci Int.* 2008, 83:207-17

[2] Kiyokage E, Kobayashi K, Toida K   *J Comp Neurol.* 2017, 525:1059–1074, **cover**

[3] Matsuno T, Kiyokage E, Toida K   *J Comp Neurol.* 2017, 525:1633-1648.

[4] Notsu E and Toida K   *Microscopy* 2019, 68:316-328.

[5] Suzuki Y, Kiyokage E, Sohn J, Hioki H, Toida K.   *J Comp Neurol.* 2015, 523:262–280

[6] Hamamoto M, Kiyokage E, Sohn J, Hioki H, Haratda T, Toida K
J Comp Neurol. 2016, 525:574–591

[7] Satoh K., Kiyokage E., Ichikawa S., Toida K   *Neurosci. Lett.* 2020, 738: 135386

[8] Horie S, Kiyokage E, Hayashi S, Inoue K, Sohn J, Hioki H, Furuta T, Toida T
J Comp Neurol. 2021 529: 2189-2208, **cover**

Figures:
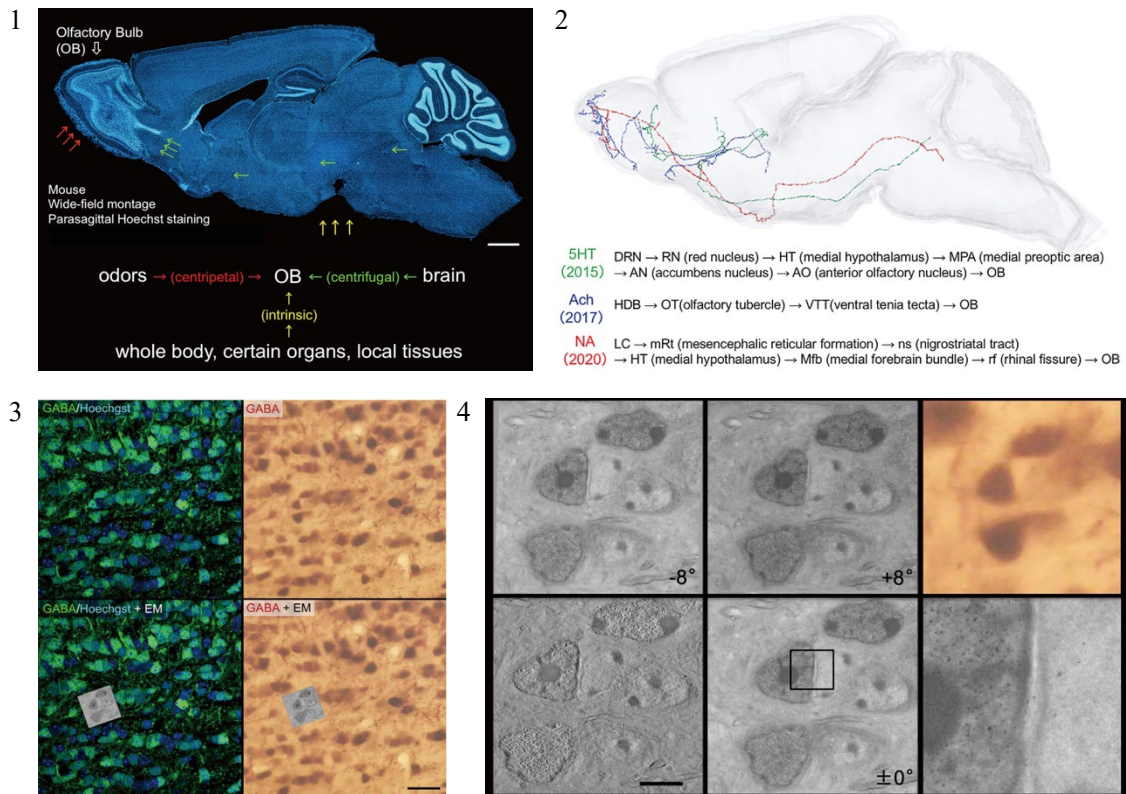
Fig.1: Para-sagittal plane of the mouse brain labeled by hoechst (blue), showing the olfactory bulb, which is regulated by multimodal, centripetal (red), centrifugal (green) and intrinsic (yellow) factors.

Fig.2: Centrifugal fibers of serotonin (5HT), acetylcholine (Ach), and noradrenaline (NA) revealed by Cre-mice and AAV.

Fig.3: Diversity of GABA- expression

Fig.4: Immunoreactivity labeled by silver-gold was analyzed by 3D-high-voltage EM.

Fig.5: EM tomography indicated variation.

17

Developmental analysis of complex synaptic connections by correlative light and electron microscopy

Shuichi Hayashi[1*], Anna Hoerder-Suabedissen[2], Nobuhiko Ohno[3,4], Emi Kiyokage[5], Catherine Maclachlan[6], Kazunori Toida[1], Graham Knott[6], Zoltán Molnár[2]

[1]Department of Anatomy, Kawasaki Medical School, Okayama, Japan, [2]Department of Physiology, Anatomy and Genetics, University of Oxford, Oxford, UK, [3]Department of Anatomy, Jichi Medical University, Tochigi, Japan, [4]Division of Ultrastructural Research, National Institute for Physiological Sciences, Aichi, Japan, [5]Department of Medical Technology, Kawasaki University of Medical Welfare, Okayama, Japan, [6]BioEM Facility, School of Life Sciences, EPFL, Lausanne, Switzerland
*s.hayashi@med.kawasaki-m.ac.jp

It remains unclear how neuronal activity regulates synaptic development. Axonal projections from layer 5 of the cerebral cortex form characteristic giant boutons in the posterior nucleus of the thalamus (Po) and provide a powerful input to thalamic neurons. To understand the 3D ultrastructure of the giant boutons and how neuronal activity is involved in their synaptic morphogenesis, we first developed correlative light and electron microscopy (CLEM) using confocal microscopy and serial block face scanning electron microscopy (SBF-SEM). Fluorescently labelled axons are correlated in fluorescent and EM images without staining (Fig. 1) [1]. We found that multiple excrescences from one Po dendrite connect with the same single layer 5 giant bouton that completely encloses them (Fig. 2A,B). We next examined the layer 5 giant boutons in *Synaptosomal-associated protein 25* (*Snap25*) conditional knockout (cKO) mice, in which regulated vesicular release at synapses of layer 5 neurons was removed [2]. The initial synapse formation in Po was not different between *Snap25*-cKO and control boutons at postnatal day 8 (P8). However, the size of the *Snap25*-cKO boutons was significantly smaller than that of control at P18. Although the *Snap25*-cKO boutons retained single synapses with the shaft of Po dendrites, no dendritic excrescences protruded into the boutons, and this caused a decrease in the total number of synapses on each *Snap25*-cKO bouton (Fig. 2C,D) [3]. We also found that deletion of *Snap25* in granule cells in the dentate gyrus of the hippocampus leads to similar synaptic defects in their axons called mossy fibers. These results suggest that regulated vesicular release is required for the maturation of the complex synaptic connections of corticothalamic projections and hippocampal mossy fibers.

References

[1] Maclachlan, C. et al., Frontiers in Neuroanatomy, 2018; 12:88

[2] Hoerder-Suabedissen, A. et al., Cerebral Cortex 2019; 29(5):2148-2159

[3] Hayashi, S. et al., Cerebral Cortex, 2021;31(5): 2625–2638
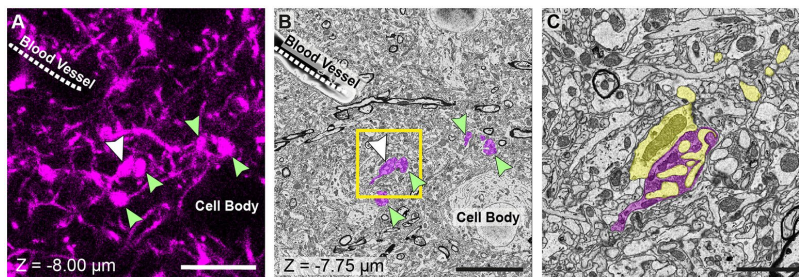
Fig. 1. Correlative light and electron microscopy of layer 5 corticothalamic axons. (A-C) Fluorescent image (A) and EM micrographs (B, C) of labelled axons. Scale bars, 10 μm in (A) and (B), 2.5 μm in (C). Modified from Maclachlan et al., 2018.
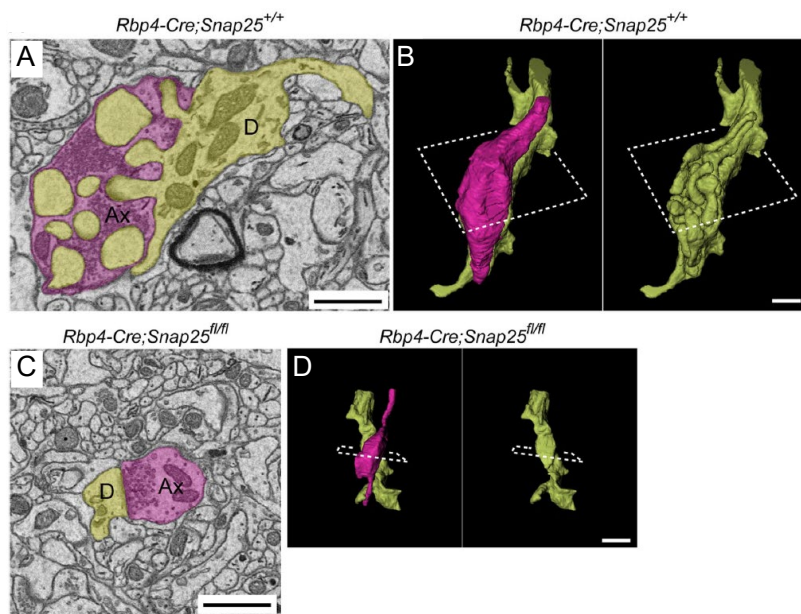
Fig. 2. SBF-SEM of layer 5 corticothalamic axonal boutons. (A,B) Wild-type. (C,D) *Snap25*-cKO. No dendritic excrescence is formed in *Snap25*-cKO brains. Scale bars, 1 μm. Modified from Hayashi et al., 2021.

Getting ahead of the next pandemic: When antibiotics stop working

Amal Seffouh[1,2] and Joaquin Ortega[1,2]

[1]Department of Anatomy and Cell Biology, McGill University, Montreal, Quebec H3A 0C7, Canada, and [2]Centre for Structural Biology, McGill University, Montreal, Quebec H3G 0B1, Canada,

Antimicrobial resistance is on track to become the next global pandemic. A recent analysis of this emerging threat predicts grim scenarios and alarming economic estimates that are not difficult to imagine while still immersed in the Covid-19 pandemic. In the last three decades, discovery efforts have been limited to generate improved versions of legacy antibiotics that target conventional vital pathways in bacterial species causing infectious diseases. Resistance to these modified drugs quickly emerges. Developing novel antibiotics that target unexplored cellular processes not susceptible to existing resistance mechanisms is urgent. Our research focuses on the assembly process of the bacterial ribosome, which is not currently targeted by any antibiotic. Ribosomes synthesize all cellular proteins. If an organism cannot make ribosomes, it dies. Ribosomes are complex molecular nanomachines made up of over 50 components. We found that critical steps within the ribosome assembly process have tremendous potential as targets for developing novel antibiotics. Our recent work identified one of these critical steps (Seffouh et al., 2019; Seffouh et al., 2022). Three proteins, RbgA, YphC and YsxC, bind to the assembly intermediate that accumulates at this step. The three proteins are essential for the 50S subunit to reach its mature state. We aim to understand how exactly RbgA, YphC and YsxC act to complete the maturation of this critical assembly intermediate and transform it into a functional 50S subunit. We use cryo-electron microscopy and single particle analysis to directly image these proteins to gain insights into how they interact with the assembling subunit and the maturation steps they catalyze. Uncovering these critical steps in the assembly process will allow leveraging ribosome biogenesis factors as a novel antimicrobial target and discovering new antibiotics that will help curve the rapidly emerging threat of antimicrobial resistance.

References:

[1] Seffouh, A., Jain, N., Jahagirdar, D., Basu, K., Razi, A., Ni, X., Guarne, A., Britton, R.A., and Ortega, J. (2019). Structural consequences of the interaction of RbgA with a 50S ribosomal subunit assembly intermediate. Nucleic Acids Res 47, 10414-10425. 10.1093/nar/gkz770.

[2] Seffouh, A., Trahan, C., Wasi, T., Jain, N., Basu, K., Britton, R.A., Oeffinger, M., and Ortega, J. (2022). RbgA ensures the correct timing in the maturation of the 50S subunits functional sites. Nucleic Acids Res. 10.1093/nar/gkac059.
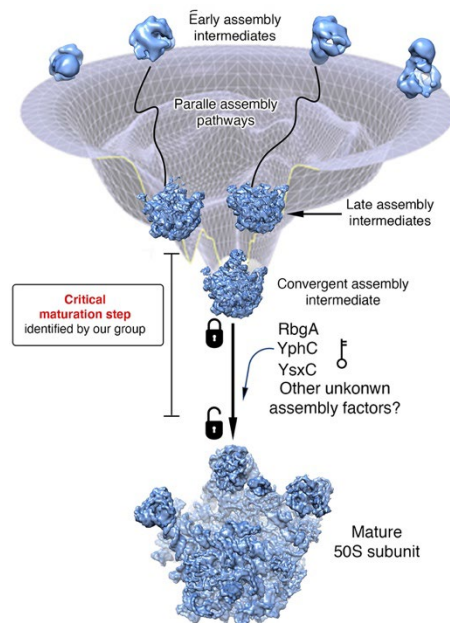
Fig. 1. Overview of the 50S subunit assembly process. Ribosomal particles at early stages of assembly follow parallel assembly pathways that converge into a critical maturation stage. The assembly intermediate that accumulates is 'locked' and its maturation is paused. RbgA, YphC and YsxC act on this intermediate to 'unlock' it and complete the maturation of the functional sites.

National and International Bioimaging Networks

Claire M. Brown[1,2*]
[1] Associate Professor, McGill University, Montreal, Quebec, Canada
[2] Advanced BioImaging Facility, McGill University, Montreal, Quebec, Canada
[*]claire.brown@mcgill.ca

Over the past decade, a number of national and international networks have emerged to support bioimaging scientists and their research. The focus of this presentation will be on two Canadian networks - the Canadian Network of Scientific Platforms its Canada BioImaging technology node, BioImaging North America and the Global BioImaging network. The Quality Assessment and Reproducibility for Instruments & Images in Light Microscopy (QUAREP-LiMi) network has leveraged these communities to improve microscope quality management and will also be discussed.

Canada BioImaging (CBI) currently has 65 members from 7 provinces and 28 institutions within Canada, and falls under two umbrellas as a technology node of the Canadian Network of Scientific Platforms (CNSP) and a geographical node of BioImaging North America (BINA). CBI and BINA share many of the same goals and objectives, with a focus on providing a welcoming and supportive community for bioimaging scientists to grow and support each other, through training and professional development activities. Both are light microscopy focused, advocating for bioimaging platforms (a.k.a. core facilities) and imaging scientists working within the platforms who make up a large proportion of their membership. The CNSP has a broader mandate and encompanses cutting edge scientific infrastructure and expertise within scientific platforms across science and engineering. The CNSP provides professional development opportunities, community engagements and advocates to funders and the Canadian government. The CNSP represents 194 scientific platforms in 45 institutions and has good representation from across Canada. Its efforts are aligned with those of CBI and

technologies and expertise they need to do high-quality science. The CNSP does focus more on aspects that apply to all technology areas and not those that apply specifically to bioimaging. For example, there is a focus on the formation of a national expertise database, development of Quality Management programs, and a general effort to develop unique metrics for measuring the impact and showcasing the importance of Scientific Platforms. BINA represents imaging scientists from the US, Canada and Mexico and its membership is currently in excess of 700 people, (88% academic, 12% corporate, 76% USA, 12% Canada, 3.2% Mexico, 9% international with an additional 16 countries represented).

Six BINA working groups, made up of volunteers, engage in activities focused on providing opportunities for interaction, education, advocacy and standardization. The BINA Quality Control and Data Management working group joined forces with QUAREP-LiMi and the broader global effort around improving quality assessment and quality control for light microscopy, spearheading the landmark FOCUS issue in Nature Methods last December [1]. This issue featured 9 articles offering guidelines and tools for improving the tracking, and reporting of microscopy metadata with an emphasis on reproducibility and data re-use. This BINA working group also developed a metrology suitcase program bringing the tools and protocols required for microscope QC to individual platforms. The Training and Education working group has worked with international stakeholders to develop a centralized repository for microscopy resources (https://microscopydb.io/). This database system is intended to be a singular central

resource for the global community making it easier to submit, find and share resources (training resources, jobs. conferences, workshops). The database is searchable and partners can access and display relevant content on their own websites.

Global BioImaging (GBI) represents a significant number of international partners including CBI and BINA (Figure 1). GBI provides a united voice for all network organizations and has working groups focused on addressing the challenges of the global community (Career Development, Demonstrating Impact). They have brought the global community together to develop a number of International Recommendations [2] such as the Impact of Imaging Facilities [3], the Added Value of Open Access Imaging Facilities [4] and Standards for Open Image Data Formats [5] to raise awareness and advocate for imaging facilities and imaging scientists. They provide training opportunities and international job shadowing to support career growth and development. GBI hosts an annual Exchange of Experience meeting to bring global network community representatives together to share ideas and strategize ways to build and strengthen the community.

In summary, the support and advocacy provided by these national and international bioimaging networks is democratizing access to advanced microscopes and expertise around the world, working to sustain the critical research infrastructure and changing the culture by highlighting the importance of imaging facilities and imaging scientists to enable successful world class science.

References: [1] Reporting and reproducibility in microscopy, Nature Methods 03 December 2021 https://www.nature.com/collections/djiciihhjh) [2] Global BioImaging International Recommendations https://globalbioimaging.org/documents [3] Added Value of Open Access Imaging Facilities [4] Impact of Imaging Facilities [5] https://pubmed.ncbi.nlm.nih.gov/33948027/
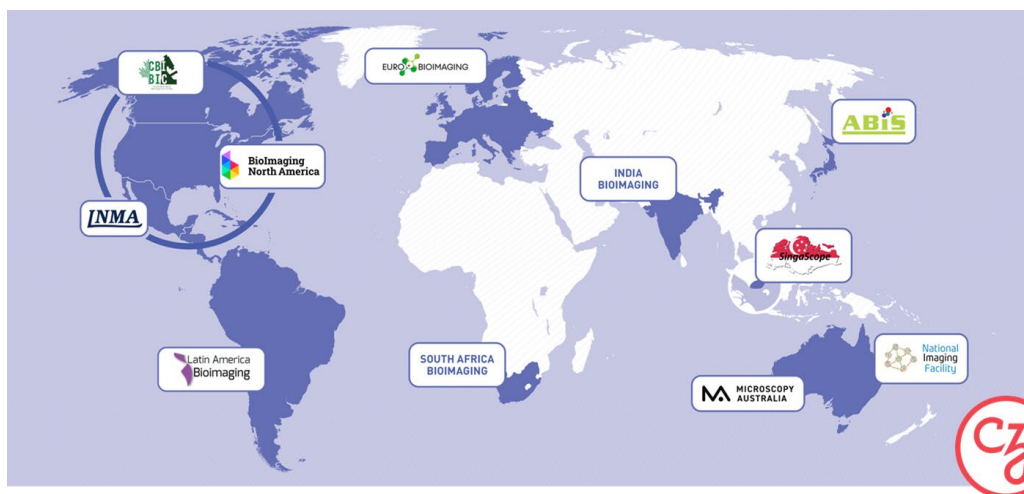
Figure 1: The Global BioImaging Network includes Euro-BioImaging, Japan's Advanced BioImaging Support, Microscopy Australia, National Imaging Facility, Mexico's National Laboratory For Advanced Microscopy, South Africa BioImaging, India BioImaging Consortium, SingaScope, Canada BioImaging, BioImaging North America and Latin America Bioimaging. Future members include: Armenia, Chile, South Korea and the African BioImaging Consortium.

Materials Science Session 1

TEM of Thick polymer or biological specimens

Ray Egerton[1*], Misa Hayashida and Marek Malac[2]

[1] Physics Department, University of Alberta, Edmonton, Canada
[2] NRC-Nano, Edmonton, Canada
*regerton@ualberta.ca

The continued development of three-dimensional electron imaging (tomography) has stimulated renewed interest in electron scattering in thick TEM specimens, and in procedures for extracting structural information from this process. A judicious choice of microscope parameters requires some knowledge of the angular distribution of electron scattering as a function of specimen thickness and incident- electron energy.

Using a 300kV TEM, we have measured the bright-field collection efficiency F and the mass-thickness contrast C (for a 10% thickness change) for carbon samples of thickness up to 750 nm [1], equivalent to a 1.4 μm of polymer of biological tissue. From these data values, the dose-limited resolution is calculated to be in the range $1 - 2$ nm for an objective-aperture semi-angle of $\beta \sim 2$ mrad and a characteristic dose of 100 e/Å^2, typical of an organic material.

Of course, radiation damage provides only one limit to spatial resolution. In fixed-beam TEM mode, chromatic aberration imposes a limit of typically 2 to 3 nm, as deduced from the chromatic point-spread function [2]; see Fig. 1. In STEM mode, the combined effect of probe diameter, beam divergence and beam broadening provide a similar limit, with an optimum convergence semi-angle $\alpha = 1 - 2$ mrad; see Fig.2. Such resolution is an order of magnitude better than that offered by optical fluorescence microscopy and is substantially better than zone-plate STXM.

References:

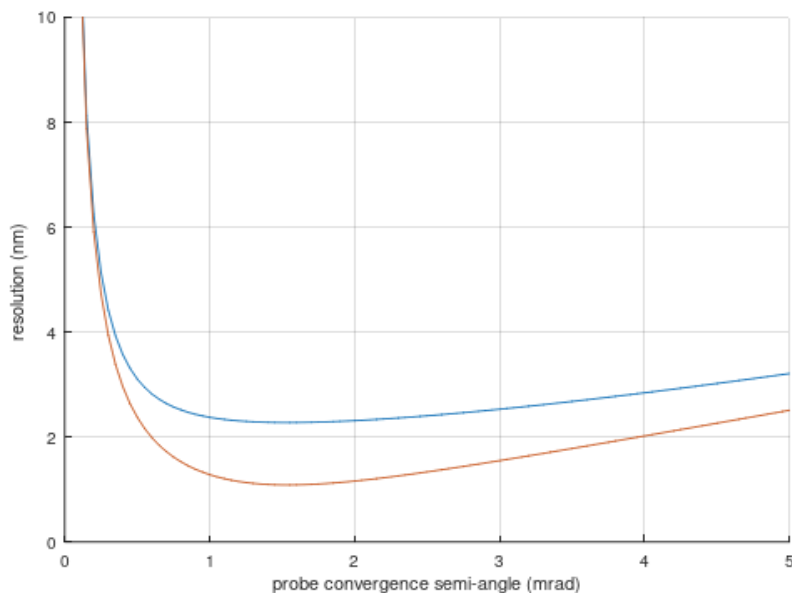[1] M. Hayashida and M. Malac , Microscopy & Microanalysis, Vol. **28**, (2022) 659-671..

[2] R.F. Egerton and M. Watanabe, Micron, Vol. **160**, (2022) 103304.
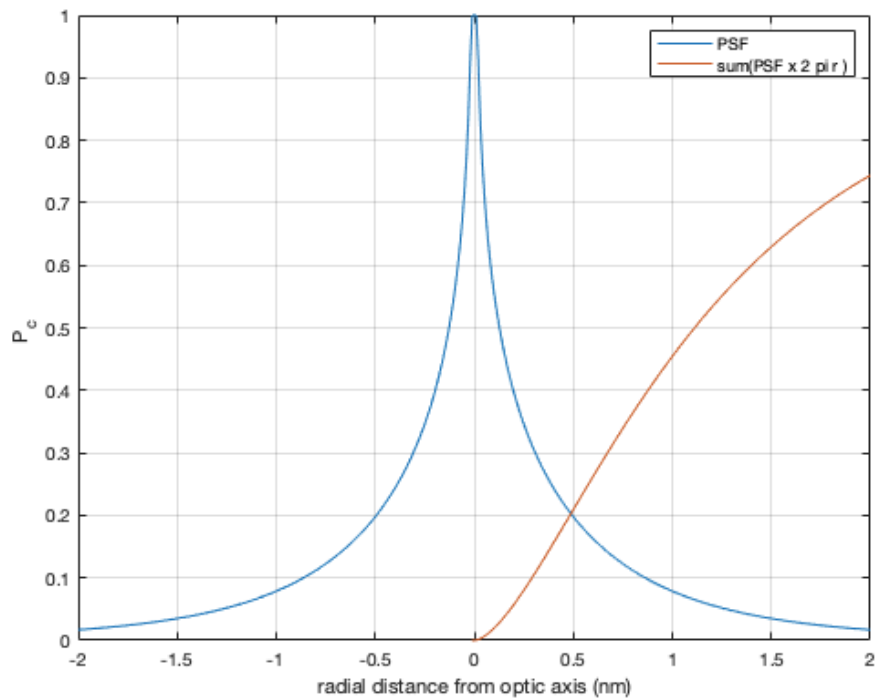
Fig. 1. Blue: chromatic-aberration PSF for 300kV TEM of 500nm-thick carbon with β = 2.4 mrad, C_c = 1.6 mm. Red: Fraction of electrons within a given radius, showing that half them lie within a diameter of 2.2 nm.

Fig. 2. 300kV STEM resolution for carbon of thickness 500 nm, plotted against probe semi-angle α, for the case of a large collection semi-angle β (blue curve), and also for $\beta = \alpha$ (red curve) - demonstrating the effect of collection-aperture collimation on the beam-broadening component.

Improving spatial resolution in rapid electron tomography for hundreds-nm-sized 3D materials

Tomohito Ishii（石井智仁）[1], Jun Yamasaki（山﨑順）[2, 3*]

[1] Department of Quantum Information Electronics, Graduate school of Engineering, Osaka University, 2-1 Yamadaoka, Suita 565-0871, Japan

[2] Research Center for Ultra-High Voltage Electron Microscopy, Osaka University, 7-1, Mihogaoka, Ibaraki, Osaka 567-0047, Japan

[3] Institute of Materials and Systems for Sustainability, Nagoya University, Furo-cho, Chikusa, Nagoya 464-860, Japan

*yamasaki@uhvem.osaka-u.ac.jp

Electron tomography is a method for measuring the three-dimensional (3D) structures and density distributions of materials smaller than 1 micron based on sequential tilt images (tilt series). For high-precision 3D reconstructions, acquisitions of about 100 micrographs at different angles are required, resulting in measurements sometimes longer than 1 hour. In addition to accumulation of irradiation damages, such a long measurement time limits the number of observations in a day's experiment, that is, the number of field of views and/or the number of sequential 3D measurements of time evolutions of materials. Recently, rapid electron tomography (RET), in which a tilt series is recorded as a movie for about 10 seconds, has been realized by a high-speed camera developed for electron beam detections [1]. However, RET often suffers from deterioration of the resolution of the reconstructed 3D volume due to vibrations of the sample holder during the high-speed tilting. Hence the objective of this study is to solve the problem to recover the original resolution in the 3D reconstruction.

In the present study, we used the high-voltage electron microscope (JEOL: JEM1000EES) of Osaka University, operated at the acceleration voltage of 1250 kV and equipped with a 1600 fps high-speed camera (Gatan: K2-IS). A tilt series of bright-field TEM images was recorded for 14 seconds as approximately 20,000 frames, while continuously tilting the sample holder from -70° to +70° at a constant rate (10°/sec). Polystyrene latex spheres and a crystalline ZnO nanoparticle were employed as the standard samples to examine the reconstruction quality.

As mentioned before, some frames in the tilt series are blurred due to the holder vibration as shown in Figs. 1(a) and (d), while others are clear as shown in Fig. 1(b) and (e) although the SNR is poor due to the short exposure time of 1600 fps. We developed a

method to quantify the image sharpness available even for flames with such poor SNRs. Based on the method, the sharpest images in each group of 16 consecutive frames (consisting of a tilt range of 0.1 degree) were selected as the representative images of each tilt ranges. The 3D reconstruction using only them shows higher resolution than that using all the frames, as shown in Fig. 2. However, since the flames other than the representatives are discarded, the SNR in the reconstructed volume becomes poor. To enhance the SNR in the representative frames, we utilized robust principal component analysis (RPCA), which is effective to separate the object image and the background noise [2], as shown in Figs. 1(c) and (f).
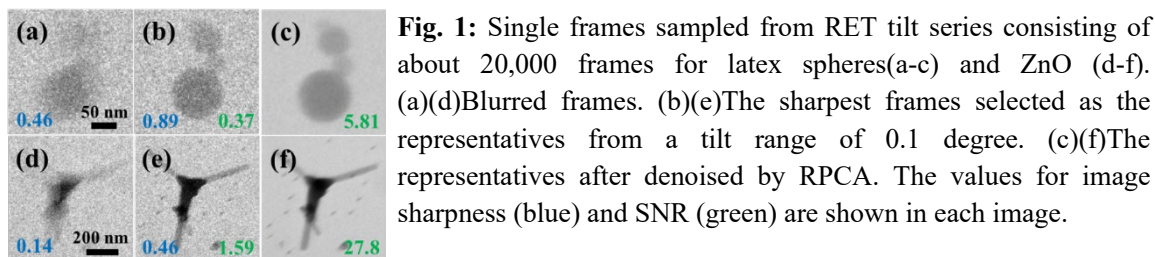
Figure 2 shows comparison of the 3D volumes of the latex spheres and ZnO nanoparticle reconstructed based on all the frames and on only the representative frames, without and with the RPCA processing. As clearly shown in Fig. 2(i), the resolution estimated from the 3D volumes has been improved by selecting the representative frames in exchange for the decrease in the SNR, which has been recovered successfully by the RPCA. Thus, the combined use of the sharp image selection and the RPCA is effective to increase the quality of the reconstructed 3D volume in RET.

References:

[1] V. Migunov, et al. Sci. Rep. **5** (2015) 14516.　　[2] E. Candes, et al, J. ACM, **58** (2011) 11.

Fig. 1: Single frames sampled from RET tilt series consisting of about 20,000 frames for latex spheres(a-c) and ZnO (d-f). (a)(d)Blurred frames. (b)(e)The sharpest frames selected as the representatives from a tilt range of 0.1 degree. (c)(f)The representatives after denoised by RPCA. The values for image sharpness (blue) and SNR (green) are shown in each image.
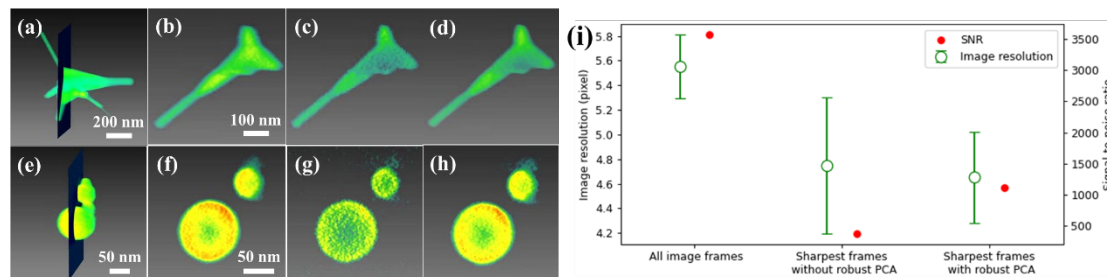
Fig. 2: Comparison of the reconstructed volumes of latex spheres(a-d) and ZnO(e-f). (a)(e) shows the slice planes. The slice images reconstructed on (b)(f) all the frames and (c)(g) only the sharpest frames, and (d)(h) after the RPCA processing. (i) Image resolution and SNR measured in the reconstructed 3D volume by FBP.

Magnetic dynamics probed by ultrafast transmission electron microscopy

Takahiro Shimojima

RIKEN Center for Emergent Matter Science (CEMS), Wako 351-0198, Japan

It has been an important issue to track the magnetic dynamics in nanometer scale, since it provides a direct evidence for the manipulation of the self-organized magnetic nanostructures, such as skyrmions[1,2], under external stimuli. The characteristic time scales for their motions are expected to be very fast which requires better time resolution for the Lorentz transmission electron microscopy (LETM) observation. A promising way to improve the time resolution of the electron microscopy is the application of the ultrafast optical pump-probe technique[3]. Previous pump-probe LTEM[4,5] studies reported the morphorogical changes of the magnetic objects with the time resolusion being independent of the camera response time (ms).

Here, we report skyrmion dynamics in defect-introduced $Co_9Zn_9Mn_2$ by using pump-probe LTEM[6]. Following the nanosecond photothermal excitation, we resolve 160-nm skyrmion's proliferation at <1 ns, contraction at 5 ns, drift from 10 ns to 4 µs, and coalescence at ~5 µs. These motions relay the multiscale arrangement and relaxation of skyrmion clusters in a repeatable cycle of 20 kHz. Such repeatable dynamics of skyrmions, arising from the weakened but still persistent topological protection around defects, enables us to visualize the whole life of the skyrmions and demonstrates the possible high-frequency manipulations of topological charges brought by skyrmions.

References:

[1] S. Mühlbauer et al., *Science* **323**, 915 (2009).

[2] X. Z. Yu et al., *Nature* **465**, 901 (2010).

[3] B. Barwick, et al., *Science* **322,** 1227 (2008).

[4] G. Berruto et al., *Phys. Rev. Lett.* **120**, 117201 (2018).

[5] M. Möller et al., *Communications Physics* **3**, 36 (2020).

[6] T. Shimojima et al., *Science Adv*ances **7**, eabg1322 (2021).

Ferroelectric nanostructures observed by transmission electron microscopy

Hiroshi Nakajima[1*] and Shigeo Mori[1]

[1] Department of Materials Science, Osaka Metropolitan University, Sakai, Osaka 599-8531, Japan. *h-nakajima@omu.ac.jp

Ferroelectrics are known as important functional materials that play various roles in electronics, various sensors, and energy harvesting applications. The functional properties depend largely on the polarization reversal caused by the movement of the boundary between domains with different polarization directions within the solid. Therefore, it is important to clarify how domain walls exist and how they move microscopically in ferroelectrics [1]. In particular, charged domain walls of ferroelectrics, in which ferroelectric polarizations face each other, have the property that the electrical conductivity changes significantly at the domain wall, even though the width is only a few nanometers. Although such unique charged domain walls have been found in some ferroelectrics, their structures are energetically unstable and thus it is an important issue to elucidate the stabilization mechanism. In the layered perovskite ferroelectric oxide $Ca_{3-x}Sr_xTi_2O_7$ ($x = 0.54$), many charged domain walls have been observed in the crystal [2], but their microscopic structure has not been clarified. In this study, we visualized the charged domain structure in $Ca_{3-x}Sr_xTi_2O_7$ ($x = 0.54$) on an atomic scale using scanning transmission electron microscopy (STEM) and clarified its structure [3].

Figure 1a shows a HAADF-STEM (High-angle annular dark-field STEM) image of a charged domain wall at $[1\bar{1}0]$ incidence. Noticeably, the crystalline domains on both sides of the charged domain wall are translating. The domain wall structure is shown in Figure 1b. The translational distance of the crystal domain corresponds to 0.1889 times the c-axis length, and such a boundary is called an out-of-phase boundary [4]. In addition, the atoms are brighter at the interface than in the interior of the crystal, suggesting elemental segregation at the interface.

Figure 2a shows a dark-field image of the observed region. In this region, linear charged domain walls are formed, indicating the existence of domain walls on a macroscopic scale. The results of elemental analysis (Fig. 2b-f) show that the Sr and Ca atomic rows face each other across the charged domain wall, which confirms the structure shown in Figure 1b. The distribution of Ti also indicates that the crystal domain is translationally shifted. Furthermore, corresponding to the strong intensity in the

HAADF-STEM image, Sr elements are segregated at the interface as indicated by the white circles.

In summary, we observed the charged domain structure by a combination of TEM dark-field method and high-resolution HAADF-STEM methods. The charged domain wall is energetically unstable due to the divergence of the electric field caused by the facing electric polarizations. As a stabilization mechanism, an out-of-phase boundary is formed in the charged domain wall. In such a structure, the electric polarization of each atom is partially parallel as indicated by the dotted lines (Fig. 1b). Therefore, such a structure is considered to make the charged domain wall more stable.

References:

[1] G. Catalan, et al., Rev. Mod. Phys. Vol. **84**, (2012) 119.

[2] Y.S. Oh, et al., Nat. Mater. Vol. **14**, (2015) 407.

[3] H. Nakajima, et al., Commun. Mater. Vol. **2**, (2021) 109.

[4] M.A. Zurbuchen, et al., J. Mater. Res. Vol. **22**, (2007) 1439.
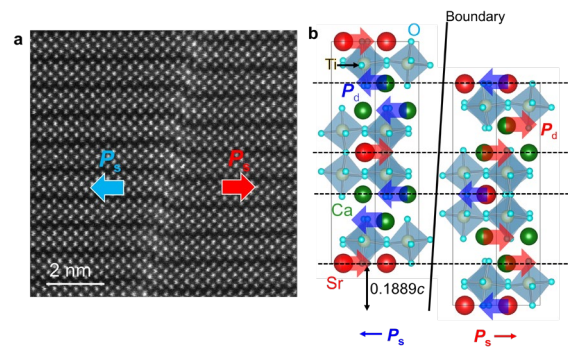
Fig. 1. Structure of a charged domain wall and its schematic. **a**. HAADF-STEM image. **b**. Crystal structure. P_s is the direction of macroscopic electric polarization. Arrows indicate the direction of displacement of each atom.
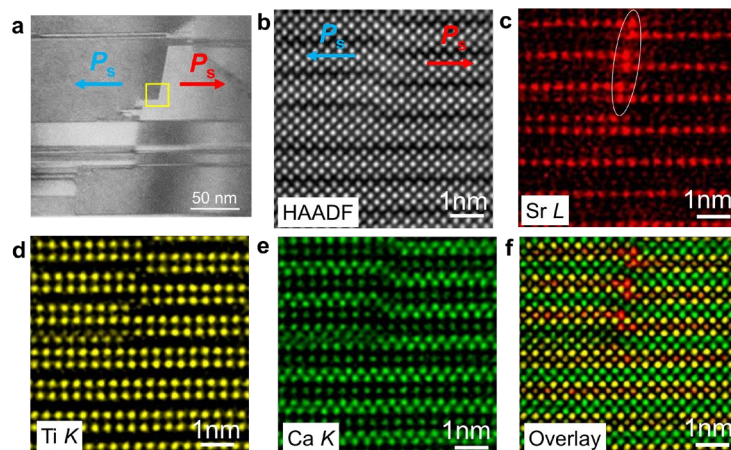
Fig. 2. Elemental analysis of charged domain wall. **a**. Dark-field image by 113 reflection. The yellow box indicates the area observed by STEM. **b-f**. EDS-STEM images at various absorption edge energies.

In-situ L-TEM observations of magnetic skyrmion and antiskyrmion dynamics

Licong Peng[1*]

[1]RIKEN Center for Emergent Matter Science (CEMS), Wako, Saitama 351-0198, Japan
[*]licong.peng@riken.jp

Magnetic skyrmions (topological "particle") and antiskyrmions ("antiparticles") hosting opposite topological numbers have attracted much interest in fields of fundamental physics and spintronics. Driving and controlling their motions promises skyrmion/antiskyrmion-based spintronic devices.

Here I will introduce the in-situ Lorentz TEM imaging of topological spin textures and their dynamical behaviors. First, I will show the manipulation of a single skyrmion at room temperature in the chiral-lattice magnet $Co_9Zn_9Mn_2$-based microdevice using nanosecond current pulses. We have directly observed the skyrmion translation and transverse Hall motion and a dynamic transition from the static pinned state to the linear flow motion via a creep event using Lorentz TEM [1]. In addition to skyrmions, I will then present the real-space control of room-temperature antiskyrmions in magnets with D_{2d} [2] and S_4 [3-4]symmetries. We have tuned the external magnetic field, temperature, thickness, and sample geometries to induce the topological transformations among the antiskyrmions, elliptical skyrmions, and non-topological bubbles via the creation, propagation, and annihilation of Bloch line pairs. We have also used the electric current to drive the antiskyrmion movement efficiently.

Figure 1 shows the single-skyrmion motion stimulated by the pulsed current in the $Co_9Zn_9Mn_2$-based microdevice at room temperature [1]. Figure 2 shows the topological transformation among antiskyrmions, skyrmions, and non-topological bubbles in magnets with D_{2d} [2] and S_4 [3-5]symmetries.

In summary, we have utilized Lorentz TEM to tune the topological nature of skyrmions/antiskyrmions, including the topological number, helicity, and lattice form, and directly observed the dynamical motions, paving a route to controlling topological spin textures with spintronic functions.

References:

[1] L. C. Peng et al. Nat. Commun., **12** (2021), 6797.

[2] L. C. Peng et al. Nat. Nanotech. **15** (2020), 181-186.

[3] K. Karube#, L.C. Peng# et al., Nat. Mater. **20** (2021), 335–340.

[4] L. C. Peng et al. Adv. Sci. (2022), 2202950.
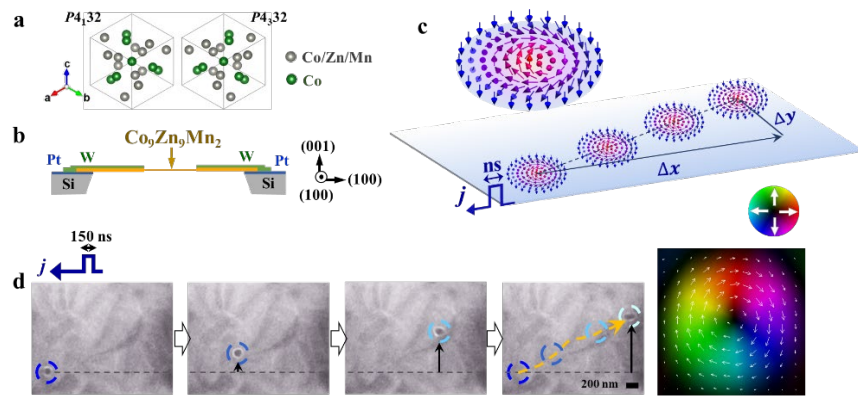
Fig. 1: (a) Crystal structure of $Co_9Zn_9Mn_2$; (b) Schematic of $Co_9Zn_9Mn_2$-based microdevice. (c) Schematic of skyrmion motion with the translational and transverse displacements induced by pulsed electric current j. (d) Over-focus L-TEM images showing the single-skyrmion motion stimulated by $j = -6.06 \times 10^{10}$ A m^{-2} pulsed current with a pulse duration of 150 ns [1].
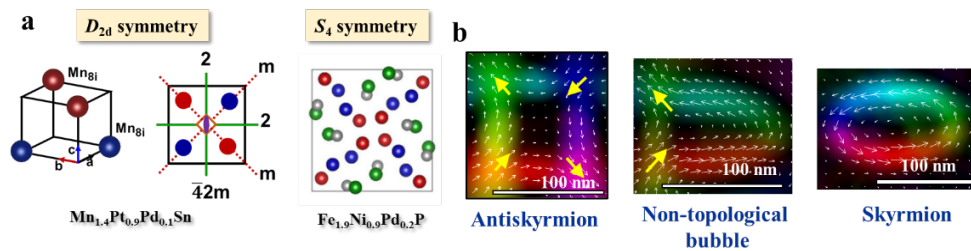
Fig. 2. (a) Crystal structure of magnets with D_{2d} [2] and S_4 [3-4] symmetries. (b) Magnetic textures of antiskyrmion, non-topological bubble, and skyrmion.

Electronic state analysis using monochromated STEM-EELS

Hiroki Kurata[1*], Takashi Nemoto[1] and Mitsutaka Haruta[1]

[1] Institute for Chemical Research, Kyoto University, Gokasho, Uji, Kyoto 611-0011, Japan.
*kurata@eels.kuicr.kyoto-u.ac.jp

Improving the energy resolution of electron energy-loss spectroscopy (EELS) with a monochromator incorporated in a scanning transmission electron microscope (STEM) is driving new research in electronic state and vibrational analyses in local regions with high spatial resolution. In order to maximize the features of high energy resolution EELS, it is necessary to acquire high quality spectrum imaging (SI) data. Recently we developed a new method to remove the dark reference of a charge coupled device (CCD) accurately [1], enabling the detection of a single signal count. Combining high-precision dark reference subtraction with multi-frame acquisition technique is very effective for measuring SI data consisting of monochromatic EELS with low signal strength. In this contribution, we will present application results of electronic state analysis using the energy-loss near-edge structure (ELNES) appeared in core-loss spectra.

Figure 1 shows the hole mapping of high-temperature superconductor of $La_{2-x}Sr_xCuO_{4\pm\delta}$ [2]. The holes are detected as the pre-peak shown by the vertical arrow in oxygen K-edge ELNES. Two-dimensional hole maps using the pre-peak intensity visualize the spatial distribution of the doped holes. The hole is preferentially doped at the oxygen site in the CuO plane in the under-doped sample of x=0.15, but the hole is also distributed at the apical oxygen sites in the over-doped sample of x=0.3. Such the two-dimensional hole mapping has been firstly realized with atomic resolution. Figure 2 shows the temperature dependence of the Ti $L_{2,3}$-edge ELNES of $SrTiO_3$. The crystal field splitting between t_{2g} and the e_g peaks narrows slightly with increasing temperature, which is attributed to the elongation of bond length between Ti and oxygen ions. The crystal field splitting decreases linearly with temperature with a slope of 0.2 meV/K as shown in Fig. 2(c). Considering the lattice expansion rate of 4 fm/K, the change of crystal field splitting due to the bond length expansion appears in the spectrum as a change of 50 meV/pm, suggesting the possibility of the measurement of sub-pm bond
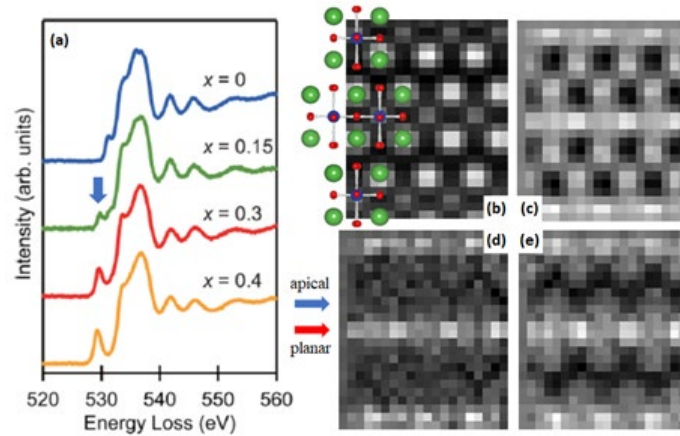
length change by ELNES. We also discuss the spectrum simulation considering the thermal vibrations.

References:

[1] M. Haruta, Y. Fujiyoshi, T. Nemoto, A. Ishizuka, K. Ishizuka and H. Kurata, Ultramicroscopy, 207, (2019), 112827.

[2] M. Haruta, Y. Fujiyoshi, T. Nemoto, A. Ishizuka, K. Ishizuka and H. Kurata, Phys. Rev. B 97, (2018), 205139.

[3] M. Haruta, T. Nemoto and H. Kurata, Appl. Phys. Lett., 119, (2021), 232901.

Figure 1 (a) Oxygen K-edge ELNES of $La_{1-x}Sr_xCuO_{1\pm\delta}$. (b) HAADF image (c) Oxygen map (d) and (e) Hole mapping for x = 0.15 and 0.3, respectively.
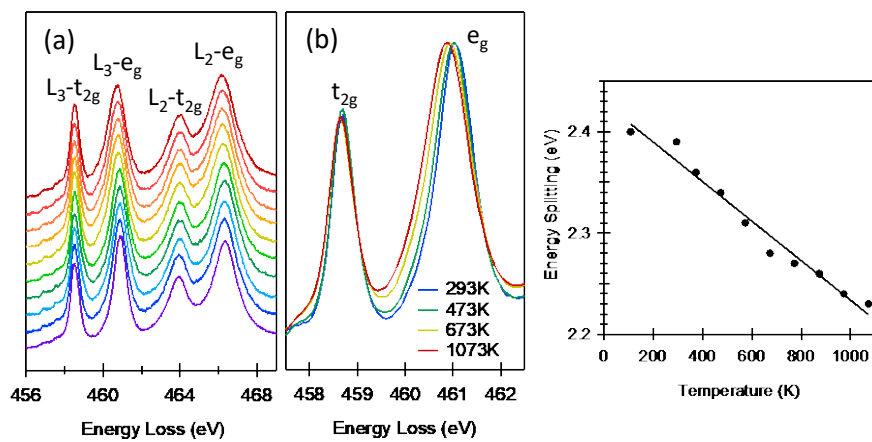
Figure 2 (a) Temperature dependence of Ti $L_{2,3}$-edge ELNES of $SrTiO_3$ (b) Enlarged L_3 peak region (c) Temperature dependence of the energy splitting between L_3-t_{2g} and L_3-e_g peaks.

Day 2 **(Tokyo time: Saturday, November 5, 2022)**

Materials Science Session 2

Accessing Sub-Ångström Ptychographic Information in a Scanning Electron Microscope Below 30 kV

Arthur M. Blackburn[1*], Cristina Cordoba[1], Matthew Fitzpatrick[1], Robert McLeod[2]

[1] Department of Physics and Astronomy, University of Victoria, 3800 Finnerty Road, Victoria, BC, V8W 2Y2, Canada.
[2] Hitachi High-Tech Canada Inc., 89 Galaxy Blvd, Etobicoke ON, M9W 6A4, Canada.
*ablackbu@uvic.ca

Advances in electron microscopy techniques and instrumentation aim to maximize the useful information given from the sample under investigation. Ideally the information is gained with minimal damage to the sample, and with minimal cost and time. From these goals there has been a long-standing to break into the high-resolution (sub-Ångström, $< 10^{-10}$ m) regime using general purpose, non-aberration corrected, low energy (< 30 keV) scanning electron microscopes. Experimentally we show that this goal is now possible.

We achieve this using a relatively simple modifications to a conventional scanning electron microscope combined with the latest generation high-speed, uncoated hybrid direct-electron detectors and recent advances in multi-slice ptychographic reconstruction algorithms. Specifically, we used a Hitachi SU9000 SEM/STEM with an additional simple projector lens; an uncoated Dectris Quadro camera; and multi-slice maximum likelihood solvers [1]. The solvers also used blurring convolution [2] on the forward projected model diffraction to help compensate for projective chromatic aberration effects.

Here, as an example, we used samples comprised of gold particles on free-standing few-layer MoS_2 and on thin amorphous carbon. Our experiments used a 20 keV beam energy and a defocused electron probe. The beam was placed at around 2000 points with a known random positional offset from a regular grid over an ~40 nm field of view. Convergent beam diffraction patterns were collected at each point. Ptychographic reconstruction, using this diffraction data, yielded a phase and amplitude transfer model of the samples (Figures 1 and 2). Their fast Fourier transforms show the presence of features below 1 Å. These features can also be seen directly in the reconstructions. In the case of the MoS_2 sample we can make direct comparisons to near identical regions of the

same sample observed at 60 kV in an aberration corrected TEM, where we see similar high-resolution information is revealed on the material.

The ability to access sub-Ångström information with a 20 keV electron beam, in a non-aberration corrected microscope changes the landscape of options for high-resolution electron microscopy. This makes it possible for a wider community to access truly high-resolution information from thin materials samples at low energies.
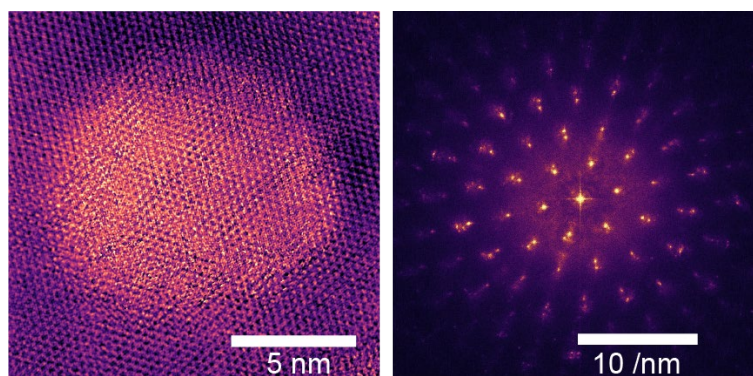
References:

[1] Z. Chen, Y. Jiang, et al., Science, Vol. **372**, (2021), 826.

[2] M. Odstrcil, J. Bussmann, et al., Optics Letters, Vol **40**, (2015), 5574.
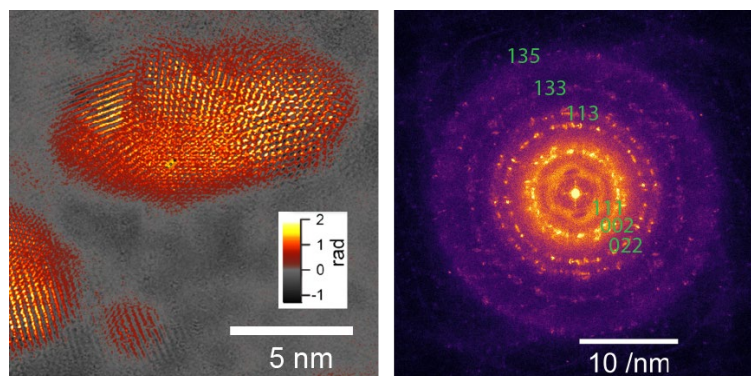
Fig. 1. Phase reconstruction of gold particle (left) and its fast Fourier transform (FFT, right) formed from 20 keV diffraction data.

Fig. 2. Mixed phase and amplitude image of an Au island on MoS_2 (left) and its FFT (right) reconstructed from 20 keV diffraction data.

Automatic Quantification of Microplastic Fibres in Scanning Electron Micrographs

Jane Howe[*], Bin Shi, Medhavi Patel, Dian Yu, and R. J. Dwayne Miller

University of Toronto, 184 College Street, Toronto, Ontario, Canada.
[*]Jane.howe@utoronto.ca

Microplastics are found everywhere, from samples in urban air to oceans of the arctic regions. It has increasingly become a problem to the environment and health of humans and other living beings. To evaluate the spread of microplastic pollution, microplastics were often examined by visible light microscopy and quantified by labor-intensive visual screening procedures. Among all shapes of microplastics, microplastic fibres, the most abundant pollution in the marine environment, are difficult to count due to their curvilinear and elongated shapes.

We first generated the scanning electron micrograph dataset of microplastic fibres (MPF) collected from various resources, which includes the SEM images and ground-truth manual segmentations [1]. We then applied two deep learning models, the classical U-Net [2] and its viable successor MultiResUNet for the semantic segmentation. The Semantic segmentation results are presented in Figure 1. Both models significantly outmatched conventional computer vision techniques and achieved a high average Jaccard index (Intersection-Over-Union, abbreviated to IoU) over 0.75. The pixel-embedding U-Net was implemented for instance segmentation on overlapping fibres, shown in Figure 2. For shape classification, MPFs are classified using a fine-tuned VGG16 neutral network with a high accuracy of 98%. With trained models, it takes only seconds to segment and classify a new micrograph in high accuracy, which is remarkably cheaper and faster than manual identification.

In summary, the proposed deep learning approaches facilitated microplastics quantification with high accuracy.

performed in part with the help of Dr. Jason Tam. This research was enabled in part by support provided by Compute Canada.

References:

[1] B. Shi, et al., Science of the Total Environment 825 (2022) 153903, and the references therein.

[2] O. Ronneberger, P. Fischer, T. Brox, International Conference on Medical image computing and computer-assisted intervention. (2015), 234–241.

Datasets	U-Net1 IoU/DSC (%)	MultiResUNet1 IoU/DSC (%)	Otsu IoU/DSC (%)
Fibre_full	78.49±1.86/87.49±1.16	**78.80±2.36/87.55±1.75**	45.47/60.99
Fibre_clean	86.74±2.14/92.80±1.33	**87.23±1.61/93.06±1.04**	54.38/70.24
Fibre_noisy	73.28±3.49/83.94±2.63	**74.30±2.87/84.74±1.99**	37.26/52.52

Fig. 1. Semantic segmentation results. MultiResUnet/U-Net with # of filters (32, 64, 128, 256, 512) achieved high overall IoU in both cropped clean/noisy (low SNRs) MPFs datasets with a 5-fold cross validation.
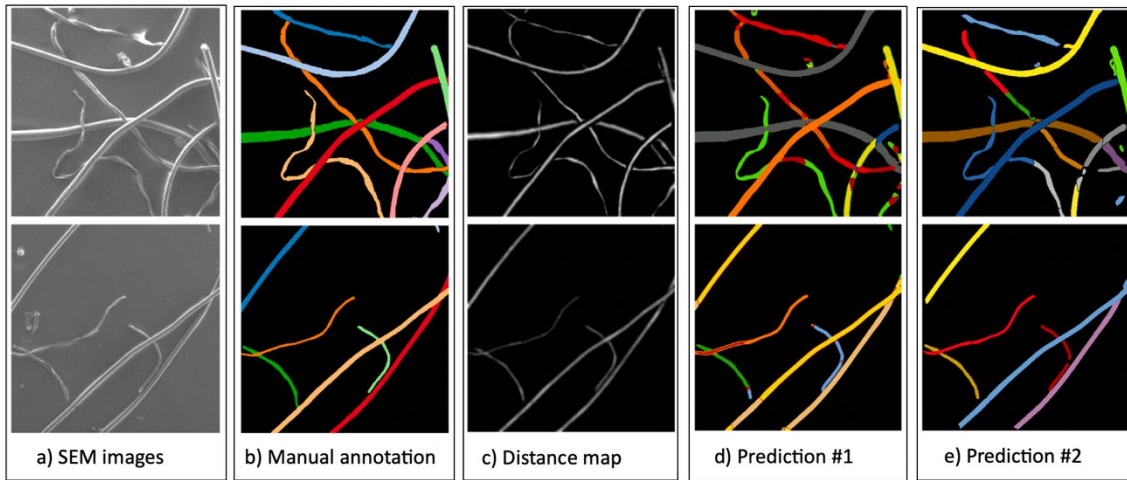
Fig. 2. Instance segmentation results. Note in (d) and (e), Mean-shift and heuristic methods were used for post processing, respectively. Different instances were labelled in different colours for counting.

Local structure analysis of interface and polar nano domains using convergent-beam electron diffraction

Daisuke Morikawa（森川大輔）[1*], Kenji Tsuda（津田健治）[2]

[1] Institute of Multidisciplinary Research for Advanced Materials (IMRAM), Tohoku University, Katahira 2-1-1, Aoba-ku Sendai, 980-8577, Japan
[2] Frontier Research Institute for Interdisciplinary Sciences (FRIS), Tohoku University, Aramaki aza Aoba 6-3, Aoba-ku, Sendai, 980-8578, Japan

Convergent-beam electron diffraction (CBED) is one of the powerful techniques for nano-meter area structural analysis. From its specific features such as nano-meter probe, dynamical scattering, and direct determination of electrostatic potential, CBED can be applied for the analysis of interfaces and in-situ observation of polar nano-domains. In this presentation, some examples for recent results obtained by CBED method are described.

Fig. 1 shows CBED patterns obtained from an area of $CaTiO_3$ containing a twin boundary. While the bulk sample of $CaTiO_3$ has a centrosymmetric structure, the twin boundary is reported to have a polar structure. CBED patterns depending on the position of the electron probe exhibit clear symmetry changes. Different types of twin boundaries were found, even though the two boundaries show the same symmetry changes. A quantitative analysis of the CBED pattern revealed a polar crystal structure at the twin boundary [1].

Fig. 2 shows a map of mirror symmetry breaking originates from the tetragonal phase of $BaTiO_3$ under an electric field. Even when applying an electric field that is high enough for switching mesoscopic polar domains, inhomogeneous distributions of rhombohedral nano domains were still observed. Three different types of nanodomain configurations in the beam direction under electric field were proposed from comparing simulated CBED patterns with inhomogeneous stacking models [2].
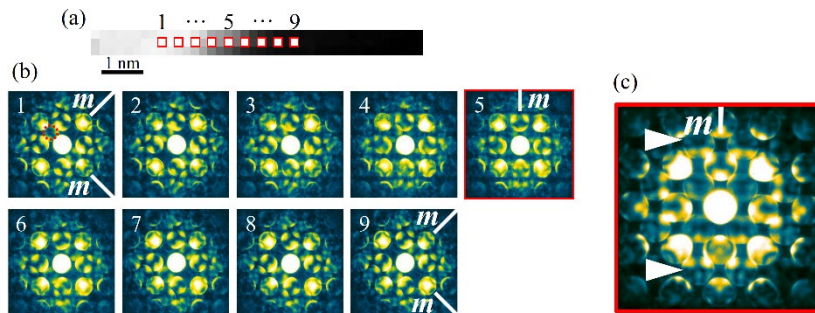
References:

[1] D. Morikawa and K. Tsuda, *Appl. Phys. Lett.*, **118**, (2021), 092901.

[2] D. Morikawa and K. Tsuda, *Appl. Phys. Lett.*, **119**, (2021), 052904.

Fig. 1. (a) Reconstructed scanning transmission electron microscopy image of a twin boundary of $CaTiO_3$ formed by summing the intensities of CBED patterns at the position indicated by the red circle in (b) 1. The STEM image was reconstructed from 40×3 CBED patterns. (b) CBED patterns obtained for the positions shown in (a) 1–9. The letter "m" denotes mirror symmetry. Position 5 corresponds to the twin boundary. (c) CBED pattern obtained at a twin boundary using an exposure time of 10 sec. and the conventional CBED mode. [1]
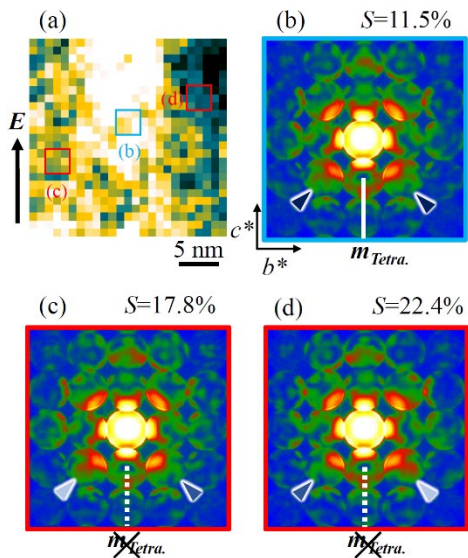
Fig. 2. (a) Symmetry-breaking index map of the tetragonal phase of $BaTiO_3$ under an electric field of 5.9 kV/cm. (b)–(d) Integrated CBED pattern from 3×3 positions shown in (a). The CBED pattern (b) shows clear mirror symmetry corresponding to the tetragonal symmetry. The pattern (c) shows a deviation from the mirror symmetry and left-right reversal relation with the pattern (d). The color arrowheads are eye-guides for understanding the difference in intensity distributions and symmetries. [2]

47

Interpretation of 3D EDX maps: multivariate analysis and deep learning hybrid approach

Frédéric Voisard[1], Ryan Gosselin[2], Jiří Dluhoš[3], Hana Tesařová[3], Vendulka Bertschová[3], Nadi Braidy[1,2*]

[1] Institut Interdisciplinaire d'Innovation Technologique 3IT, Université de Sherbrooke, 3000 Boul. de l'Université Québec, J1K 0A5, Canada Department of Chemical and

[2] Biotechnological Engineering, Université de Sherbrooke, 2500 Boul. de l'Université, Quebec, J1K 2R1 Canada

[3] Tescan Orsay Holding, a.s., 21 Libusina trida, Brno 62300, Czech Republic

[*]nadi.braidy@usherbrooke.ca

Serial sectioning tomography (SST) in the focused ion beam-scanning electron microscope (FIB-SEM)[1] constitutes an extremely powerful tool to capture subsurface microstructure in three dimensions. When coupled to energy-dispersive spectral mapping (EDS), FIB-SEMs can generate analytical information of the sampled volume. However, despite day-long acquisition times, low signal-to-noise ratio forces to choose between spectral precision and spatial resolution. In addition, simple window integral algorithms are inappropriate to appreciate the complex and rich data generated by EDS-SST. On one hand, multivariate analyses can certainly tackle the data complexity but not the load. On the other hand, the low signal-to-noise level severely impedes the generation of an acceptable training dataset for deep learning. There is therefore an opportunity to leverage the capability of multivariate analyses algorithm to classify low SNR data to produce the training dataset for the deep learning step. Here, we test this idea using a multi-phasic tribological coating made of tungsten carbides in an iron aluminide matrix. The coating was deposited using high-velocity oxyfuel jet of a ball-milled powder containing 30 % vol WC in Fe_3Al powder.

The multi-modal 3D data set was collected on an area of $51.4 \times 51.4 \times Z$ μm^3 with X-ray maps collected using 1000 channels between 0-10 keV and 728×817 pixel sampling and 186 slices using a TESCAN AMBER FIB-SEM equipped with a backscattered electron detector (BSE) and an Oxford Ultim100 X-ray detector. Each EDS frame took approximately 6 minutes. The polyphasic and porous nature of the sample makes the sole BSE image segmentation difficult via simple thresholding methods. A typical X-ray map (Fig. 2a) shows the presence of at least 5 phases, with phases sharing similar elements. In a first attempt to use deep learning, a training set was performed manually by thresholding the BSE signal and using the 4 EDS maps. 4 phases were used, believed

to represent Al_2O_3, Fe_3Al, W/WC as well as a "pore" phase. The 3D reconstruction of the classified voxels was found rough, with many areas mislabeled by manual selection error.

In a second attempt, the training dataset was produced using a hierarchal classification scheme[2] of the EDS dataset from 8 slices that greatly facilitated the identification of 8 endmembers. Using the endmembers, we could calculate abundance map for each slice by loglikelihood maximization[3] which was converted to an 8-phase mask for each BSE slice. These segmented BSE slices were then used as the training dataset for a deep learning step (3-level U-net) using Dragonfly. In this case, additional details are much clearer and helps streamline the interpretation (Fig. 2c).

References:

1. Berger, S. D. *et al.* DualBeam metrology: a new technique for optimizing 0.13-um photo processes. in (ed. Sullivan, N. T.) 423 (2001). doi:10.1117/12.436768.

2. Fauteux-Lefebvre, C. *et al* R. *Anal Chem* **90**, 13118–13125 (2018).

3. Lavoie, F. B., *et al. Chem. Int. Lab. Sys. C*, 40–50 (2016).
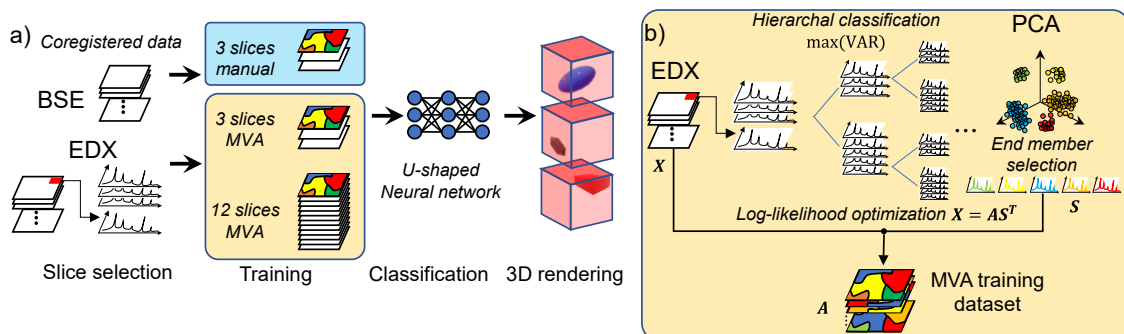
Fig. 1. (a) Algorithms for segmentation. (b) Details of the hierarchal classification to generate multivariate analysis (MVA) training dataset
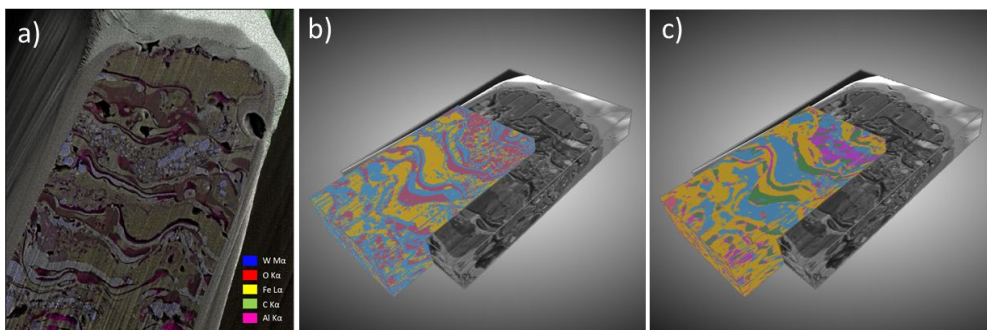
Fig. 2. (a) EDX map of a slice over BSE image (b) Machine learning segmentation from manual selection (c) U-Net deep learning segmentation using H-MCRLLM as training data

Atomic Resolution Magnetic Field Imaging by Scanning Transmission Electron Microscopy

Naoya Shibata[1,2,3*]

[1] Institute of Engineering Innovation, The University of Tokyo, Tokyo 113-8656 Japan

[2] Nanostructures Research Laboratory, Japan Fine Ceramic Center, Nagoya 456-8587, Japan

[3] Quantum-Phase Electronics Center (QPEC), The University of Tokyo, Tokyo 113-8656, Japan.

[*]shibata@sigma.t.u-tokyo.ac.jp

Aberration-corrected scanning transmission electron microscopy (STEM) is a powerful technique for directly observing atomic-scale structures inside materials and devices. However, in ordinary STEM, atomic-resolution observation of magnetic materials is essentially very difficult, since high magnetic fields (>2T) are inevitably exerted on samples inside the magnetic objective lens. We have succeeded in developing a new magnetic objective lens system that realizes a magnetic field free environment at the sample position. Using this new objective lens system combined with the state-of-the-art higher order aberration corrector, sub-Å spatial resolution in magnetic-field-free condition is realized by STEM [1]. This novel electron microscope (Magnetic-field-free Atomic Resolution STEM: MARS) is expected to be useful for research and development of advanced magnetic materials and steels.

On the other hand, by using elaborate detectors such as segmented or pixelated detectors in STEM, we can not only image atoms, but can also image electromagnetic field distribution inside samples through differential phase contrast (DPC) imaging techniques [2]. Applying DPC imaging in atomic resolution STEM, we can now directly visualize the electric field distribution within single atoms [3], i.e. the electric field between the positively charged atomic nucleus and the negatively charged electron cloud. Therefore, it becomes tempting to directly observe magnetic fields at atomic resolution by MARS. However, to visualize magnetic fields at atomic scale, we must solve remaining major difficulties even after magnetic-field-free atomic-resolution STEM imaging becomes possible. One major difficulty is that both the specimen's electric and magnetic fields inevitably contribute to the phase shift of the incident electron probe. To visualize magnetic fields, we must differentiate between electric and magnetic phase shift components in the atomic-resolution DPC images. The other major difficulty is that the

phase shift induced by the atomic-scale magnetic field is predicted to be extremely small. Thus, very high signal-to-noise ratio imaging conditions should be fulfilled. We have demonstrated that the real-space visualization of intrinsic magnetic fields of an antiferromagnetic material is possible by combining kernel filtering and unit-cell averaging techniques to solve the difficulties of differentiating between electric and magnetic phase shift components and extremely small magnetic phase shifts (Figure 1) [4]. The details of this magnetic-field-free STEM and the atomic-scale imaging of magnetic fields will be presented in the talk.

References:

[1] N. Shibata *et al.*, *Nature Comm.* **10**, 2380 (2019).

[2] N. Shibata *et al.*, *Nature Phys.*, **8**, 611-615 (2012).

[3] N. Shibata *et al.*, *Nature Comm.* **8**, 15631 (2017).

[4] Y. Kohno *et al.*, *Nature* **602**, 234-239 (2022).
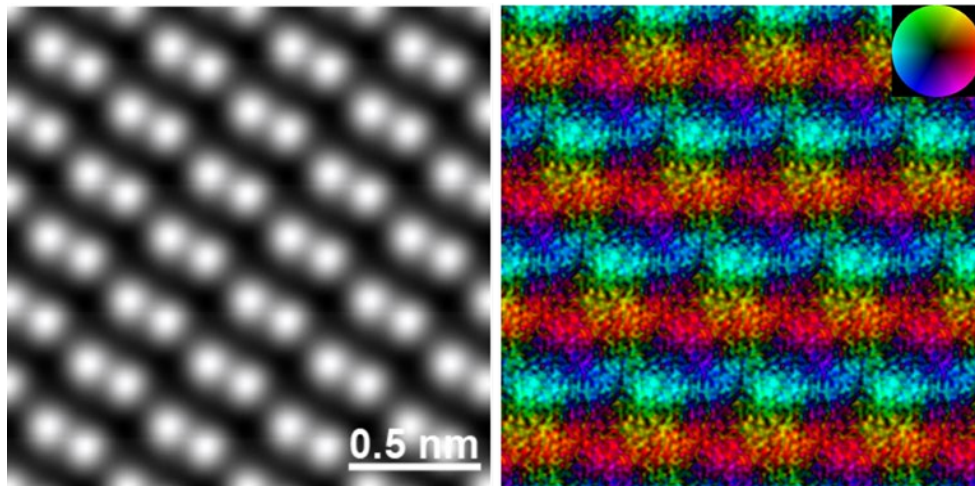
Fig. 1. (left) Unit cell averaged and tiled ADF image of α-Fe$_2$O$_3$ observed along the [$\bar{1}\bar{1}$20] direction. (right) The corresponding projected magnetic field vector color map. The antiparallel magnetic field component on the adjacent Fe-Fe double atomic layers is clearly observed, visualizing antiferromagnetic order in this crystal [4].

【Organizers】

Shigeo Mori (Osaka Metropolitan University)

森　茂生　　（大阪公立大学）

Kazunori Toida (Kawasaki Medical School, Osaka University)

樋田一徳　　（川崎医科大学、大阪大学）

Ken Harada (RIKEN)

原田　研　　（理化学研究所）

Marek Malac
　(National Research Council Canada, University of Alberta)

Misa Hayashida (林田美咲)

　(National Research Council Canada)

【Venue Information】

Kawasaki Sukenobu Memorial Lecture Hall,
Located in Kawasaki University of Medical Welfare.
https://w.kawasaki-m.ac.jp/language/english/
Matsushima 288, Kurashiki, Okayama 701-0193, Japan

From Okayama station to Nakasho station,
JR Sanyo line: approx. 15 minutes.
JR Hakubi line: approx. 13 minutes.

From Kurashiki station to Nakasho station,
JR Sanyo line: approx. 6 minutes.
JR Hakubi line: approx. 6 minutes.
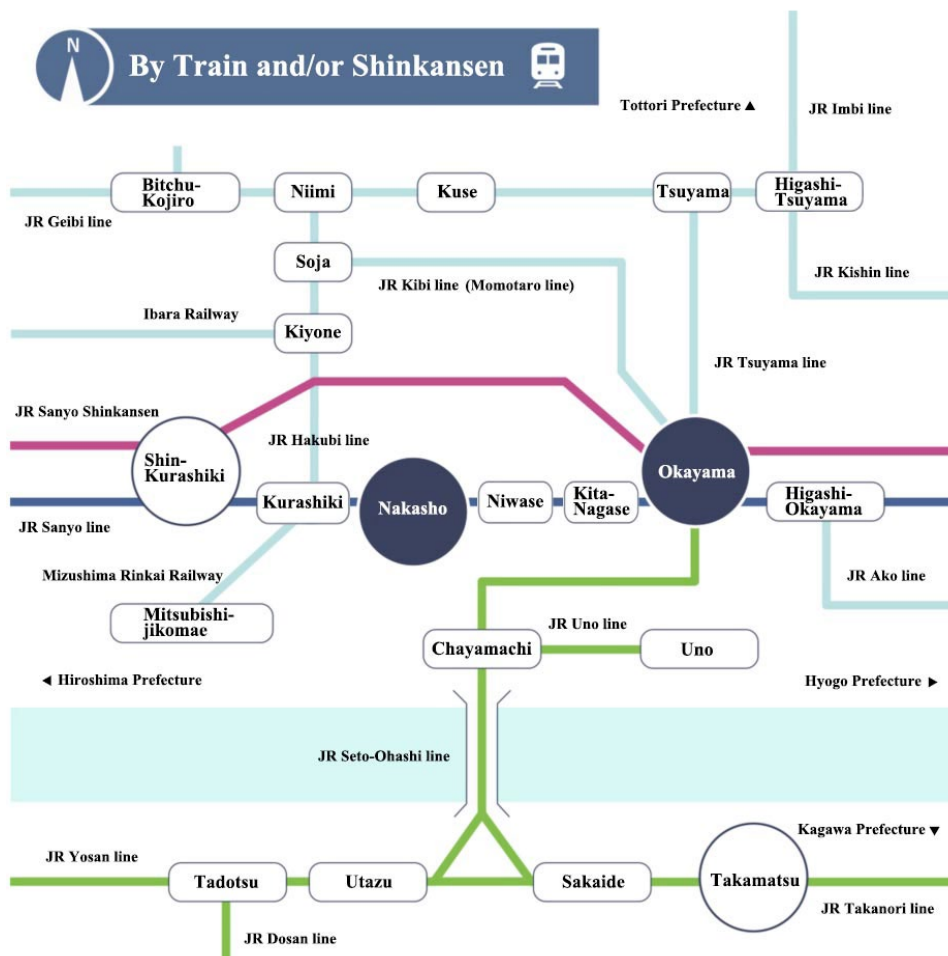
From Nakasho St. to Kawasaki University of Medical Welfare
Walk: approx. 10 minutes.

Map 1 (Nakasho area)

- Supermarket Halows
- Staff parking (P)
- Memorial Hall
- Kawasaki University of Medical Welfare
- Bas stop
- Prefectural road 162
- Tomato bank
- Police box
- Bas stop
- Kawasaki Medical School & Kawasaki Medical School Hospital
- Gym
- To Kurashiki
- Nakasho
- To Okayama
- JR Sanyo line

Map 2 (Campus)

- Parking
- Kids garden
- Athletic track
- Tennis court
- Kawasaki Sukenobu Memorial Lecture Hall
- Ground
- Kawasaki University of Medical Welfare
- Parking
- Heliport
- Gym
- Gym
- Museum
- Gym
- Parking
- Hospital
- Garden
- Kawasaki College of Allide Health Professions
- Kawasaki Medical School

Map 3 (Floor plan)

Kawasaki Sukenobu Memorial Lecture Hall

- Gallery
- Lobby
- Memorial hall
- Lobby
- Lobby
- Multipurpose hall
- Entrance
- Courtyard
- Lobby

55